Mutations in the gene encoding filamin B disrupt vertebral segmentation, joint formation and skeletogenesis

Deborah Krakow[1–3,21], Stephen P Robertson[4,21], Lily M King[2], Timothy Morgan[4], Eiman T Sebald[1], Cristina Bertolotto[2], Sebastian Wachsmann-Hogiu[5], Dora Acuna[2], Sandor S Shapiro[6], Toshiro Takafuta[7], Salim Aftimos[8], Chong Ae Kim[9], Helen Firth[10], Carlos E Steiner[11], Valerie Cormier-Daire[12], Andrea Superti-Furga[13], Luisa Bonafe[13], John M Graham Jr[2,14], Arthur Grix[15], Carlos A Bacino[16], Judith Allanson[17], Martin G Bialer[18], Ralph S Lachman[2,19], David L Rimoin[2,14,20] & Daniel H Cohn[2,14,20]

The filamins are cytoplasmic proteins that regulate the structure and activity of the cytoskeleton by cross-linking actin into three-dimensional networks, linking the cell membrane to the cytoskeleton and serving as scaffolds on which intracellular signaling and protein trafficking pathways are organized (reviewed in refs. 1,2). We identified mutations in the gene encoding filamin B in four human skeletal disorders. We found homozygosity or compound heterozygosity with respect to stop-codon mutations in autosomal recessive spondylocarpotarsal syndrome (SCT, OMIM 272460) and missense mutations in individuals with autosomal dominant Larsen syndrome (OMIM 150250) and the perinatal lethal atelosteogenesis I and III phenotypes (AOI, OMIM 108720; AOIII, OMIM 108721). We found that filamin B is expressed in human growth plate chondrocytes and in the developing vertebral bodies in the mouse. These data indicate an unexpected role in vertebral segmentation, joint formation and endochondral ossification for this ubiquitously expressed cytoskeletal protein.

Morphogenesis in vertebrate organisms requires the integration of extracellular signals with alterations in the cellular cytoskeleton. Filamins regulate the organization of cytoskeletal F-actin into either parallel bundles or orthogonal gel networks[3] and also mediate interactions between subcortical actin networks and transmembrane receptors to modulate cell-cell, cell-matrix and intracytoplasmic signal transduction[1,2,4]. Mammals have three filamin genes, *FLNA*, *FLNB* and *FLNC*. *FLNA* and *FLNB* seem to be ubiquitously expressed[5,6]; *FLNC* is predominantly expressed in muscle. Human filamin genes are highly similar with conserved exon-intron structure, and there is ~70% homology at the protein level[2,7]. The filamin monomer comprises an N-terminal actin binding domain (ABD) followed by a series of 24 β-sheet repeats that collectively bind many cytoplasmic and transmembrane proteins[1,2]. Filamins exist *in vivo* as dimers. Dimerization, leading to homo- and possibly heterodimer formation, is mediated by interactions between C-terminal sequences[5,8,9]. Mutations in *FLNA* produce a spectrum of X-linked malformation and osteochondrodysplasia syndromes. *FLNA* loss-of-function mutations are usually embryonically lethal in males and underlie a neuronal migration disorder in females[10]. Mutations producing structural changes in the protein lead to numerous developmental anomalies in the brain, skeleton and viscera[11].

Recently the gene associated with SCT, an autosomal recessive disorder characterized by short stature and vertebral, carpal and tarsal fusions[12,13], was localized on chromosome 3p14 (ref. 14). These studies and further recombination mapping (data not shown) identified a 4.7-cM candidate region, which included a 1.4-Mb region of homozygosity containing 14 genes. Mutations were not found in the candidate genes *WNT5A*[14], *ASB14* and *IL17RD* (also known as *SEF*) in affected individuals from the linked families. The gene *FLNB* localizes to this interval and, considering the role of *FLNA* in skeletogenesis[11], we looked for mutations in *FLNB* in four unrelated families with SCT.

[1]Department of Obstetrics and Gynecology and [2]Ahmanson Department of Pediatrics, Cedars-Sinai Research Institute, 8700 Beverly Blvd., Los Angeles, California 90048, USA. [3]Department of Obstetrics and Gynecology, David Geffen School of Medicine at UCLA, Los Angeles, California, USA. [4]Department of Paediatrics and Child Health, University of Otago, Dunedin, New Zealand. [5]MIST Institute, Cedars-Sinai Research Institute, Los Angeles, California, USA. [6]Department of Physiology, Jefferson Medical College, Philadelphia, Pennsylvania, USA. [7]Department of Clinical and Laboratory Medicine, Yamanashi Medical University, Yamanashi, Japan. [8]Northern Regional Genetics Service, Auckland, New Zealand. [9]Instituto da Criança, Faculdade de Medicina da Universade São Paulo, Brazil. [10]Department of Medical Genetics, Addenbrookes Hospital, Cambridge, UK. [11]Medical Genetics Department, Medical Sciences School, State University of Campinas, Campinas, São Paulo, Brazil. [12]Département de Génétique Médicale, Hôpital Necker-Enfants Malades, Paris, France. [13]Division of Molecular Paediatrics, Centre Hospitalier Universitaire Vaudois, Lausanne, Switzerland. [14]Department of Pediatrics, David Geffen School of Medicine at UCLA, Los Angeles, California, USA. [15]The Permanente Medical Group, Sacramento, California, USA. [16]Department of Molecular and Human Genetics, Baylor College of Medicine, Houston, Texas, USA. [17]Eastern Ontario Regional Genetics Program, Ottawa, Canada. [18]Department of Pediatrics, Schneider Children's Hospital at North Shore/NYU Medical Center, Manhasset, New York, USA. [19]Department of Radiology, David Geffen School of Medicine at UCLA, Los Angeles, California, USA. [20]Department of Human Genetics, David Geffen School of Medicine at UCLA, Los Angeles, California, USA. [21]These authors contributed equally to this work. Correspondence should be addressed to D.K. (deborah.krakow@cshs.org) or S.P. (stephen.robertson@stonebow.otago.ac.nz).
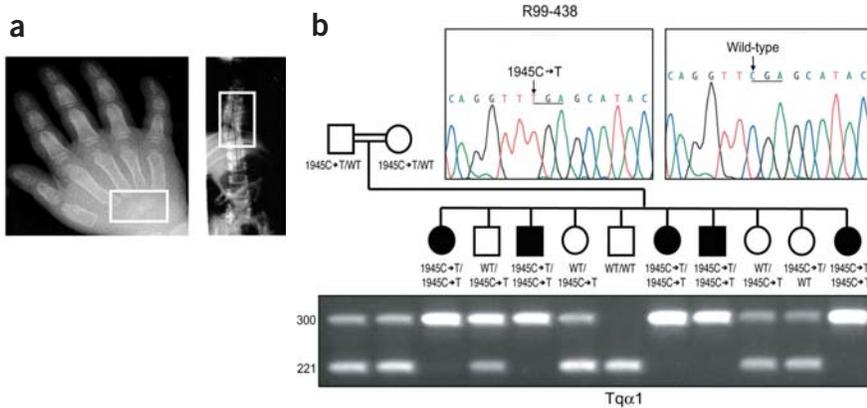
Figure 1 Mutations in *FLNB* in SCT. (**a**) Radiographs of the hand and spine of an individual in family R00-008, with boxed areas showing fusions of the capitate and hamate (left) and vertebral bodies T6–T10 (right), respectively. (**b**) Family R99-438. Chromatographs show the mutation together with a normal sequence. Below, the pedigree and a gel photograph of restriction endonuclease digestion products of PCR-amplified DNA from exon 13 shows segregation of the mutation in the family. Fragment sizes (in bp) are listed on the left and the restriction endonuclease used is indicated. WT, wild-type.

Individuals with SCT were either homozygous or compound heterozygous with respect to mutations in *FLNB* that resulted in stop codons (**Fig. 1** and **Table 1**). Affected individuals in the consanguinous family R00-008 were homozygous with respect to the mutation 6408delC that predicts a translational frameshift and a stop codon four codons downstream. Affected individuals from two additional consanguinous families (R99-438 and R03-062) were homozygous with respect to mutations (1945C→T and 7029T→G) predicted to create translational termination codons (R649X and Y2343X, respectively; **Fig. 1**). In one nonconsanguinous family (R00-084), the affected individual was compound heterozygous with respect to two mutations that predicted premature translation terminations at codons 818 and 1607. In all four families, the segregation of the mutations was compatible with the autosomal recessive inheritance pattern of SCT. All mutations found to underlie SCT predict premature stop codons within the repeat domain of filamin B, and we therefore conclude that SCT results from absence or truncation of filamin B.

We next explored whether other skeletal dysplasias with vertebral fusions were associated with mutations in *FLNB*. Larsen syndrome is a genetically heterogeneous disorder characterized by multiple joint dislocations, craniofacial abnormalities and accessory carpal bones[15–17] (**Fig. 2**). A gene associated with an autosomal dominant form of the disorder was localized to 3p21.1–14.1 (ref. 18). We studied four individuals with sporadically occurring Larsen syndrome and one family with a dominantly inherited form of the condition. We found heterozygosity with respect to missense mutations in *FLNB* that arose *de novo* in all five families (**Fig. 2** and **Table 1**). Two mutations are predicted to lead to the amino acid substitutions F161C and E227K in the ABD of filamin B. Three other mutations

predict a single amino acid deletion or substitution (1571delN, G1586R, G1691S) in repeats 14 and 15 of the protein.

AOI and AOIII are autosomal dominant lethal skeletal dysplasias with vertebral abnormalities, disharmonious skeletal maturation, poorly modeled long bones and joint dislocations[19] (**Fig. 3**). The overlap of some of these clinical and radiographic features with Larsen syndrome[20,21] prompted us to look for mutations in *FLNB* in individuals with these conditions. We identified mutations in *FLNB* in all three individuals with AOI and both individuals with AOIII that we studied (**Fig. 3** and **Table 1**). All subjects were unrelated, and the phenotype arose sporadically in their families. The three individuals with AOI were heterozygous with respect to point mutations in *FLNB* that predicted single residue substitutions in the ABD. One individual with AOIII was heterozygous with respect to the same point mutation (604A→G) identified in an individuals with AOI. Analysis of the available parental samples showed that one mutation associated with AOI and both mutations associated with AOIII occurred *de novo*. It has been suggested that Boomerang dysplasia is allelic with AOI[22], but we found no mutations in *FLNB* in one individual with this diagnosis.

The diversity of skeletal abnormalities caused by mutations in *FLNB* indicate a central role for filamin B in skeletal morphogenesis. The presence of vertebral abnormalities (block fusions, vertebral hypoplasia, malsegmentation and clefting, posterior arch hypoplasia or aplasia) prompted us to examine expression of filamin B in mouse embryos by immunostaining. We observed intense, uniform filamin B expression in condensing chondrocytes within vertebral bodies in sectioned embryos at embryonic day 14 (E14; **Fig. 4**). Reduced expression was evident in developing intervertebral discs. Additionally, there were
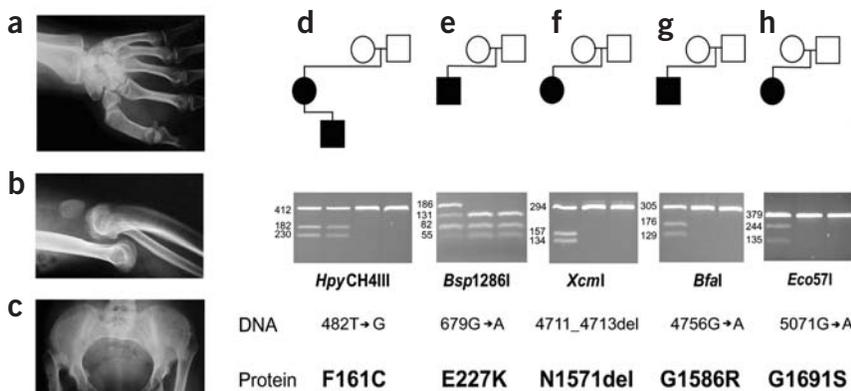
Figure 2 Mutations in *FLNB* are associated with Larsen syndrome. (**a–c**) Skeletal abnormalities in Larsen syndrome include supernumerary carpal bones and dislocations of the large joints, such as the knees and hips. (**d–h**) Pedigrees and restriction endonuclease digests show *de novo* mutations predicted to lead to amino acid substitutions in filamin B. The identities of the restriction endonucleases, the DNA mutation and the predicted protein sequence changes are shown below. Fragment sizes (in bp) are listed on the left.
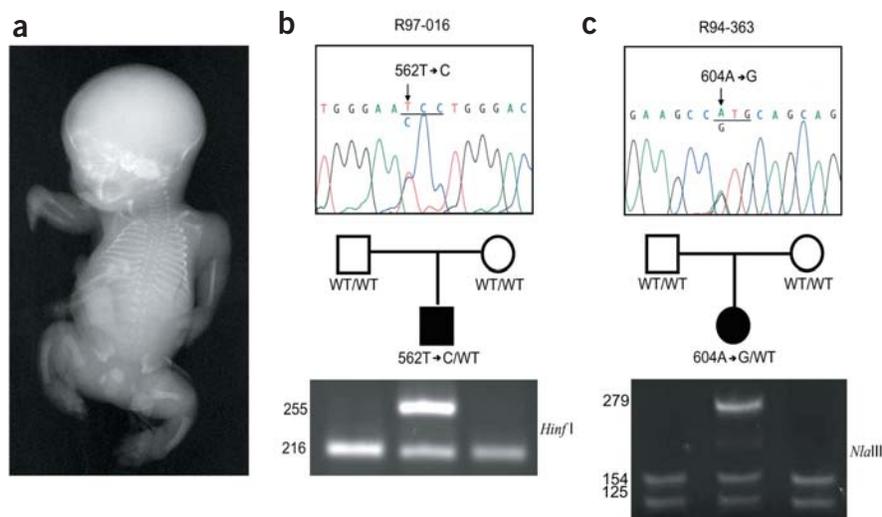
Figure 3 Mutations in *FLNB* in AOI and AOIII. (**a**) Anterior-posterior radiograph of an individual with AOI (from family R97-016) showing multiple skeletal abnormalities, including absent humeri, left radius, fibulae, hypoplastic femurs, absent thoracic vertebral bodies, a small thorax and lack of mineralization of the phalanges of the hands and feet. (**b**,**c**) Chromatographs show normal and mutated nucleotides in AOI (family R97-016) and AOIII (family R94-363),which are indicated by an arrow. The reading frame is underlined. The pedigrees and gel photographs of restriction endonuclease digestion products of PCR-amplified DNA from exon 3 show that mutations are *de novo*. Fragment sizes (in bp) are listed on the left and the restriction endonucleases used are indicated. WT, wild-type.

detectable levels of filamin B in the kidney, lung, colon and cerebral periventricular region, as reported previously[23].

The presence of short stature, epiphyseal delay and disharmonious bone mineralization in the group of disorders associated with mutations in *FLNB* suggest a role for filamin B within the epiphyseal growth plate. Some mutations in *FLNA* also affect stature and skeletal mineralization. We examined sections of normal fetal distal femur by immunofluorescence using antibodies directed against filamin A and filamin B. Filamin B was uniformly present throughout the growth plate, with expression detected in resting, proliferating, prehypertrophic and hypertrophic chondrocytes (**Fig. 5a**). In contrast, there was intense filamin A expression in chondrocytes in the hypertrophic zone, but diminished expression in resting and proliferating chondrocytes. Both filamins were localized to the cytoplasm, but in hypertrophic chondrocytes, filamin B was concentrated at the cell membrane whereas filamin A was distributed throughout the

cytoplasm (**Fig. 5a**). In proliferating chondrocytes undergoing cell division, both filamins, but especially filamin B, were concentrated at the cleavage furrow between the dividing cells (**Fig. 5b**).

The demonstration that mutations in *FLNB* (**Supplementary Fig. 1** online) are associated with a spectrum of autosomal dominant and recessive skeletal dysplasias indicates that Larsen syndrome, AOI and AOIII are genetically related conditions and adds SCT to the allelic series. Like mutations in *FLNA*[11], mutations in *FLNB* produce a diversity of phenotypes, depending on the nature and location of the mutation. The premature termination mutations underlying SCT could lead to nonsense-mediated decay[24] and absence of filamin B, but production of a stable truncated protein lacking a dimerization domain cannot be ruled out. Cell lines from the families with SCT were not available, and so these hypotheses could not be distinguished.

Dominant missense mutations in *FLNB* underlie Larsen syndrome, AOI and AOIII, disorders characterized by joint dislocation,

Table 1 Clinical findings and mutations in diseases associated with *FLNB*

|		Family Phenotypic findings							Mutation			
Diagnosis	ID#	Craniofacial abnormalities	Vertebral fusions	Vertebral abnormalities	Carpal or phalangeal abnormalities	Tarsal abnormalities	Joint dislocations	Other congenital abnormalities[a]	DNA mutations	Exon	Protein consequence	Protein ABD or repeat
SCT	R99-438	+	+	+	+	+	–	+	1945C→T	13	R649X	5
SCT	R03-062	+	+	–	+	–	–	–	7029T→G	43	Y2343X	22
SCT	R00-084	–	–	–	+	–	–	–	2452C→T	16	R818X	6
									4819C→T	28	R1607X	14
SCT	R00-008	–	+	+	+	–	–	–	6408delC	39	S2137fs	20
Larsen	319	+	–	+	+	+	+	–	482T→G	2	F161C	CHD2
Larsen	380	+	–	–	+	+	+	–	679G→A	4	E227K	CHD2
Larsen	318	+	–	+	+	+	+	–	4711_4713delAAT	28	1571delN	14
Larsen	334	+	–	+	U	U	+	–	4756G→A	29	G1586R	14
Larsen	225	+	U	U	+	U	+	–	5071G→A	31	G1691S	15
AOI	R95-326	U	–	+	+	U	–	–	518C→T	2	A173V	CHD2
AOI	R96-320	+	+	+	U	–	+	–	604A→G	3	M202V	CHD2
AOI	R97-016	+	–	+	+	U	+	–	562T→C	3	S188P	CHD2
AOIII	R83-120	+	+	+	+	+	+	–	2251G→C	15	G751R	6
AOIII	R94-363	+	–	+	+	+	+	–	604A→G	3	M202V	CHD2

[a]Other congenital abnormalities include rarefication of the retinal vessels. U, unknown; CHD2, calponin homology domain 2; fs, frameshift.
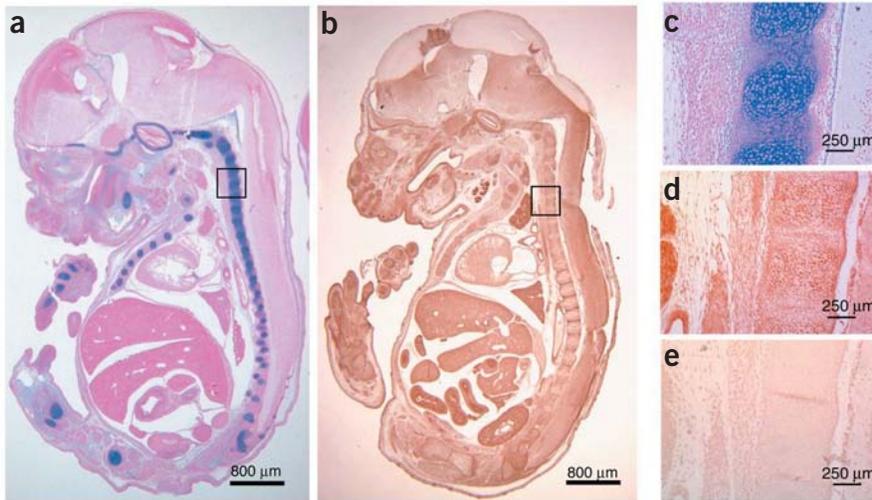
Figure 4 Distribution of filamin B in the E14 mouse embryo. (**a**) Sagittal section stained with alcian blue to detect chondrocytes. Nuclei were stained with nuclear fast red. (**b**) Sagittal section interrogated with antibody to filamin B and counterstained with hematoxylin. Brown regions correspond to filamin B staining. (**c**) Boxed area from **a** showing alcian blue staining of chondrocytes in the developing vertebral bodies corresponding to the region with high levels of filamin B shown in **d**. (**d**) Boxed area from **b** showing high levels of filamin B in chondrocytes of the developing vertebral bodies. (**e**) Negative control for the filamin B antibody staining of an E14 mouse embryo sagittal section. Area of the vertebral body corresponding to the boxed area from **b**.

implicating filamin B in joint morphogenesis. Three of the four mutations associated with AOI or AOIII occurred in the ABD, altering residues conserved among human paralogs, orthologous filamins from other species and other actin-binding proteins (**Supplementary Fig. 2** online). The presence of the same mutation (604A→G) in individuals with AOI and AOIII, conditions previously separated on grounds of radiology and chondro-osseus histology[19], suggests that such distinctions do not reflect differences in their primary molecular pathogenesis.

Three mutations producing Larsen syndrome (3 of 5 independent cases) altered conserved residues within repeats 14 and 15. Whether these predicted substitutions disrupt specific binding interactions is unclear, as interacting partners for filamin B have not been identified for these repeat elements. As with disease phenotypes associated with mutations of the ABD of filamin A[11], the severity of the disease associated with ABD substitutions in the filamin B is varied. Some well conserved residues corresponding to predicted helical components of the protein (A173V, M202V) produced lethal AOI or AOIII,
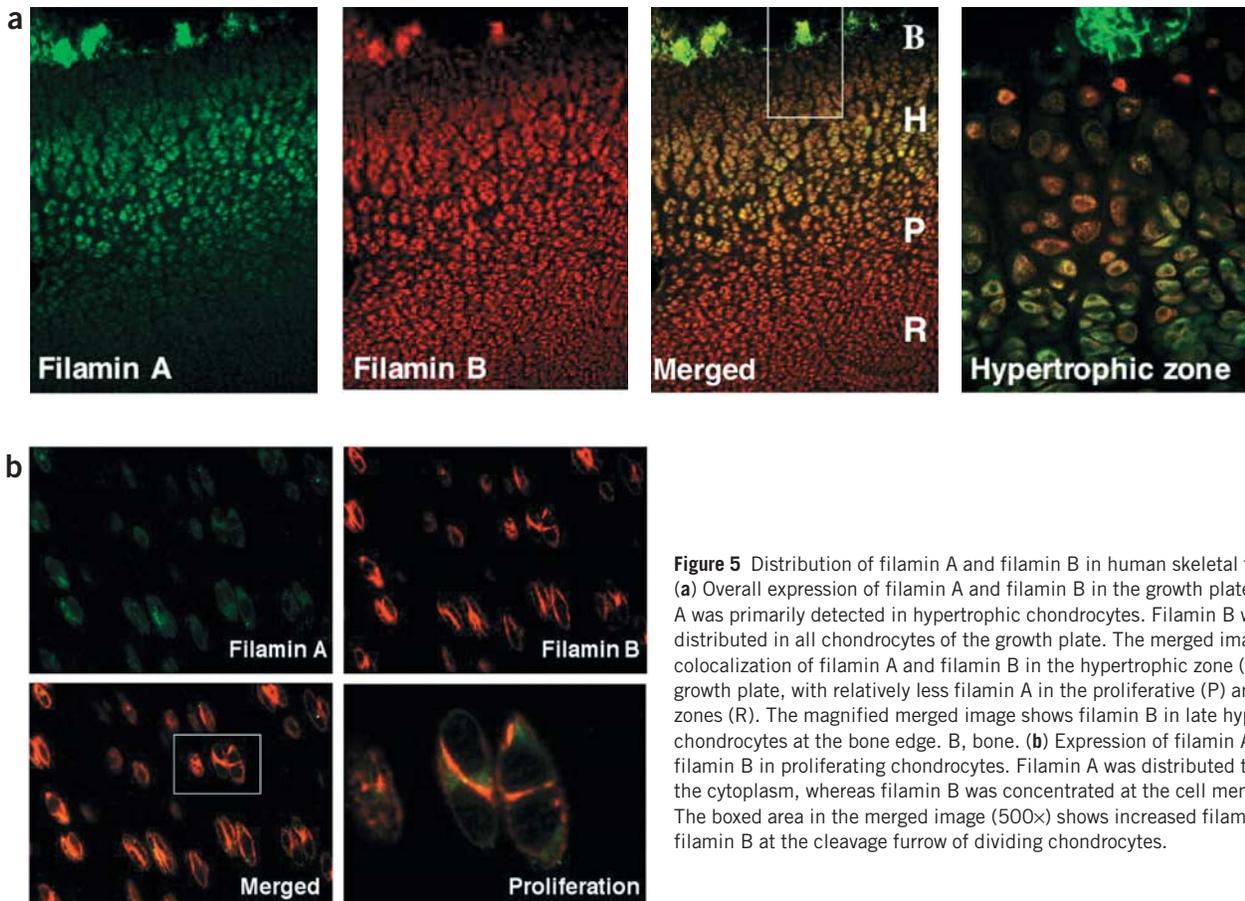
Figure 5 Distribution of filamin A and filamin B in human skeletal tissue. (**a**) Overall expression of filamin A and filamin B in the growth plate. Filamin A was primarily detected in hypertrophic chondrocytes. Filamin B was distributed in all chondrocytes of the growth plate. The merged image shows colocalization of filamin A and filamin B in the hypertrophic zone (H) of the growth plate, with relatively less filamin A in the proliferative (P) and resting zones (R). The magnified merged image shows filamin B in late hypertrophic chondrocytes at the bone edge. B, bone. (**b**) Expression of filamin A and filamin B in proliferating chondrocytes. Filamin A was distributed throughout the cytoplasm, whereas filamin B was concentrated at the cell membrane. The boxed area in the merged image (500×) shows increased filamin A and filamin B at the cleavage furrow of dividing chondrocytes.

and substitution of a conserved residue distant from the major helices (F161C) produced Larsen syndrome. Whether a structural perturbation or alteration of an extrinsic interaction with filamin B underlies these effects awaits clarification.

Female carriers of null mutations in *FLNA* manifest a neuronal migration disorder, periventricular nodular heterotopia[10]. Although both *FLNA* and *FLNB* are expressed in the periventricular region of the brain[23], we are not aware of individuals with SCT who have seizures or other evidence for anomalous neuronal migration, indicating that presumptive loss-of-function mutations in *FLNB* do not have the same biological consequence as similar mutations in *FLNA*.

The demonstration of highly localized expression of filamin B in the cartilaginous condensations of developing vertebrae has not been previously appreciated and, together with the defects in vertebral development observed in individuals with mutations in *FLNB*, indicates a pivotal role for the protein in vertebral patterning and morphogenesis. In cartilage, distinct expression patterns for filamin A and filamin B indicate different roles for these proteins. Coexpression of the two proteins in hypertrophic chondrocytes suggests possible functional redundancy for the proteins in these cells, but there seems to be a distinct role for filamin B in the remainder of the growth plate. The histology of the growth plate in AOI and AOIII includes a diminished chondrocyte population and widespread acellular islands in the resting zone, sometimes containing cell remnants or multinucleated giant cells[19]. The observation of filamin B concentrated at the cleavage furrow of dividing chondrocytes may indicate that some mutations in *FLNB* confer a defect in cell division that leads to formation of multinucleated giant cells and possibly accelerated apoptosis, resulting in hypocellularity in the resting zone of the growth plate. Understanding the specific mechanisms by which *FLNB* mutations produce defects in skeletal morphogenesis and abnormalities in other organ systems will be facilitated by the findings described here. This will include the identification of specific filamin B binding partners and the pathways and downstream signal transduction targets that interact with this cytoskeletal protein during development.

METHODS

Linkage analysis. Under a protocol approved by the institutional review board, we obtained informed consent from all affected and unaffected individuals in the families studied. We collected blood and extracted DNA by standard protocols. Recombination mapping used the markers at the loci *D3S2400*, *D3S3616*, *D3S1295*, *D3S1592*, *D3S2452*, *D3S1313* and *D3S1234*. Each 15-μl PCR contained 25 ng of genomic DNA, 200 μM dNTPs, 0.33 μM each primer, 0.5 U of Ampli*Taq* Gold DNA polymerase (PE Biosystems) and 1.5 mM MgCl$_2$. PCR was carried out using a Perkin Elmer 9700 GeneAmp Thermocycler as follows: 10 min at 95 °C; 35 cycles of 94 °C for 30 s, 55 °C for 75 s and 72 °C for 15 s; and 10 min at 72 °C. We resolved PCR products by capillary electrophoresis using an ABI model 3100 automated DNA sequencer. We analyzed genotypes using the ABI Genotyper 2.5 software package. In each family, haplotypes were created by parsimony.

Mutation detection in *FLNB*. We amplified genomic DNA fragments by PCR using a Perkin Elmer 9700 GeneAmp Thermocycler. Primer sequences and conditions are available on request. We detected mutations using denaturing high performance liquid chromatography (Transgenomic) and subsequent automated sequence analysis or by direct sequence analysis alone. We subjected amplified fragments to sequence analysis using the ABI Prism Big Dye version 3 sequencing kit (Applied Biosystems) and separated the products by electrophoresis using an ABI model 377 automated DNA sequencer. We processed the sequence data using ABI software and analyzed it using Sequencher (Gene Codes). We confirmed mutations by bidirectional sequencing. After identifying a mutation in an affected individual, we carried out segregation analysis in families by sequence analysis, restriction endonuclease cleavage or single-strand conformation polymorphism

analysis. We confirmed declared parental relationships by the segregation of four unlinked microsatellite markers (data not shown).

Antibody detection in mouse embryos. We removed the paraffin from sections of mouse embryos (Novagen) and hydrated them through a series of xylene and alcohol washes. Antigen retrieval was carried out by standard microwave citrate methods and then quenched in 0.3% H$_2$O$_2$ for 30 min. We blocked slides in 10% goat serum, 1% bovine serum albumin, 0.5% Triton in phosphate-buffered saline (PBS) for 30 min at room temperature and then incubated them with a 1:200 dilution of antibody to filamin B directed against the H1 epitope[6] in 10% goat serum, 1% bovine serum albumin, 0.5% Triton in PBS overnight at 4 °C. We stained slides with immunoperoxidase using the Vectastain ABC Elite Kit (Vector Laboratories) and mounted them in Permount (Fisher Scientific). For alcian blue staining, we stained the mouse E14 section with 1% Alcian blue (Sigma) in 3% acetic acid for 45 min and counterstained it for 5 min with 0.1% nuclear fast red (Biomedical Specialties) in 5% aluminum sulfate. We dehydrated the slides with alcohol and xylene washes and then mounted them in Permount. We analyzed the results with an Olympus Fluoview confocal microscope (Scientific Instruments Company). We captured images with an Apogee KX-2E digital camera (Apogee Instruments) and processed them with an Image-Pro, Focus Control computer program for a PC computer (Scientific Instruments Company).

Growth plate immunofluorescence. We fixed the distal fetal femur from a normal 20-week-old fetus in formalin and then decalcified it in 3% EDTA diluted in 0.1 M PBS. We cut 70-μm sections using a vibratome, blocked sections for 1 h in 5% donkey or goat serum in 0.1% Triton in PBS and then incubated them with a primary monoclonal antibody to filamin A (Neomarkers) and/or a polyclonal antibody to filamin B, each at a 1:200 dilution in 5% serum in PBS, at 4 °C for 3 d. We washed sections, treated them with either Alexa Fluor 488–conjugated donkey antibody to mouse IgG or Alexa Fluor 568–conjugated goat antibody to rabbit IgG (Molecular Probes) at a 1:200 dilution in 5% normal serum in PBS at room temperature for 1 h. We washed the sections and mounted them on slides using VECTASHIELD (Vector Laboratories) with DAPI. Duplicates of each section were incubated with PBS instead of the primary antibody as a negative control. We analyzed sections using a fluorescence microscope as described above and with a Leica TCS SP confocal microscope (Leica Microsystems).

Note: Supplementary information is available on the Nature Genetics website.

1. Stossel, T.P. *et al.* Filamins as integrators of cell mechanics and signaling. *Mol. Cell Biol.* **2**, 138–145 (2001).
2. Van der Flier, A. & Sonnenberg, A. Structural and functional aspects of filamins. *Biochim. Biophys. Acta* **1538**, 99–117 (2001).
3. Niederman, R., Amrein, P.C. & Hartwig, J. Three-dimensional structure of actin filaments and of an actin gel made with actin-binding protein. *J. Cell Biol.* **96**, 1400–1413 (1983).
4. Loy, C.J., Sim, K.S. & Yong, E.L. Filamin-A fragment localizes to the nucleus to regulate androgen receptor and coactivator functions. *Proc. Natl. Acad. Sci. USA* **100**, 4562–4567 (2003).
5. Gorlin, J.B. *et al.* Human endothelial actin-binding protein (ABP-280, nonmuscle filamin): a molecular leaf spring. *J. Cell Biol.* **111**, 1089–1105 (1990).

6. Takafuta, T., Wu, G., Murphy, G.F. & Shapiro, S.S. Human β-filamin is a new protein that interacts with the cytoplasmic tail of glycoprotein Ibα. *J. Biol. Chem.* **273**, 17531–17538 (1998).

7. Chakarova, C. *et al.* Genomic structure and fine mapping of the two human filamin gene paralogues FLNB and FLNC and comparative analysis of the filamin family. *Hum. Genet.* **107**, 597–611 (2000).

8. Sheen, V.L. *et al.* Filamin A and filamin B are co-expressed within neurons during periods of neuronal migration and can physically interact. *Hum. Mol. Genet.* **11**, 2845–2854 (2002).

9. Himmel, M., Van Der Ven, P.F., Stocklein, W. & Furst, D.O. The limits of promiscuity: isoform-specific dimerization of filamins. *Biochemistry* **42**, 430–439 (2003).

10. Fox, J.W. *et al.* Mutations in filamin 1 prevent migration of cerebral cortical neurons in human periventricular heterotopia. *Neuron* **21**, 1315–1325 (1998).

11. Robertson, S.P. *et al.* Localized mutations in the gene encoding the cytoskeletal protein filamin A cause diverse malformations in humans. *Nat. Genet.* **33**, 487–491 (2003).

12. Honeywell, C., Langer, L. & Allanson, J. Spondylocarpotarsal synostosis with epiphyseal dysplasia. *Am. J. Med. Genet.* **109**, 318–322 (2002).

13. Steiner, C.L., Torriani, M., Norato, D.Y. & Marques-de-Faria, A.P. Spondylocarpotarsal synostosis with ocular findings. *Am. J. Med. Genet.* **91**, 131–134 (2000).

14. Steiner, C.E. *et al.* A locus for spondylocarpotarsal synostosis syndrome at chromosome 3p14. *J. Med. Genet.* (in the press).

15. Larsen, L.J., Schottdstaedt, E.R. & Bost, F.C. Multiple congenital dislocations associated with characteristic facial abnormality. *J. Pediatr.* **37**, 574–584 (1950).

16. Latta, R.J., Graham, C.B., Aase, J., Scham, S.M. & Smith, D.W. Larsen's syndrome: a skeletal dysplasia with multiple joint dislocations and unusual facies. *J. Pediatr.* **78**, 291–298 (1971).

17. Marques, M.J. Larsen's syndrome: clinical and genetic aspects. *J. Genet. Hum.* **28**, 83–88 (1980).

18. Vujic, M. *et al.* Localization of a gene for autosomal dominant Larsen syndrome to chromosome region 3p21.1-14.1 in the proximity of, but distinct from, the COL7A1 locus. *Am. J. Hum. Genet.* **57**, 1104–1113 (1995).

19. Sillence, D., Worthington, S., Dixon, J., Osborn, R. & Kozlowski, K. Atelosteogenesis syndromes: a review, with comments on their pathogenesis. *Pediatr. Radiol.* **27**, 388–396 (1997).

20. Nishimura, G., Horiuchi, T., Kim, O.H. & Sasamoto, Y. Atypical skeletal changes in otopalatodigital syndrome type II: phenotypic overlap among otopalatodigital syndrome type II, boomerang dysplasia, atelosteogenesis type I and type III, and lethal male phenotype of Melnick-Needles syndrome. *Am. J. Med. Genet.* **73**, 132–138 (1997).

21. Schultz, C., Langer, L.O., Laxova, R. & Pauli, R.M. Atelosteogenesis type III: long term survival, prenatal diagnosis, and evidence for dominant transmission. *Am. J. Med. Genet.* **83**, 28–42 (1999).

22. Wessels, M.W. *et al.* Prenatal diagnosis of boomerang dysplasia. *Am. J. Med. Genet.* **122**, 148–154 (2003).

23. Sheen, V.L. *et al.* Mutations in the X-linked filamin 1 gene cause periventricular nodular heterotopia in males as well as in females. *Hum. Mol. Genet.* **10**, 1775–1783 (2001).

24. Maquat, L.E. Nonsense-mediated RNA decay in mammalian cells: A splicing-dependent means to down-regulate the levels of mRNAs that prematurely terminate translation. in *Translational Control of Gene Expression* (Sonenberg, N., Hershey, J.W.B. & Mathews, M.B. eds.) 849–868 (Cold Spring Harbor Press, Cold Spring Harbor, New York, 2000).